Structural disordering induced by electron irradiation in quasi-one-dimensional blue bronze $K_{0.3}MoO_3$

2004 J. Phys.: Condens. Matter 16 9001

(http://iopscience.iop.org/0953-8984/16/49/015)

INSTITUTE OF PHYSICS PUBLISHING JOURNAL OF PHYSICS: CONDENSED MATTER

J. Phys.: Condens. Matter **16** (2004) 9001–9012 PII: S0953-8984(04)86279-9

Structural disordering induced by electron irradiation in quasi-one-dimensional blue bronze $K_{0.3}MoO_3$

Di Yin, Jianbo Wang[1], Renhui Wang, Jing Shi and Huamin Zou

Department of Physics, Wuhan University, Wuhan 430072, People's Republic of China
and
Centre for Electron Microscopy, Wuhan University, Wuhan 430072, People's Republic of China

E-mail: wang@whu.edu.cn (Jianbo Wang)

Received 16 September 2004, in final form 2 November 2004
Published 26 November 2004
Online at stacks.iop.org/JPhysCM/16/9001
doi:10.1088/0953-8984/16/49/015

Abstract

The structural transformation of the quasi-one-dimensional charge-density-wave (CDW) conductor $K_{0.3}MoO_3$ blue bronze upon electron irradiation is reported. Evidence of the disappearance of Bragg spots corresponding to the C-centre symmetry is clearly demonstrated by the *in situ* recorded selected area electron diffraction (SAED) patterns in the transmission electron microscope, which acts as the electron irradiation facility as well as the structural analysis and recording instrument. Based on the experimental results and the crystal structure of $K_{0.3}MoO_3$ (Graham and Wadsley 1966 *Acta Crystallogr.* **20** 93), a hypothetical atomic model is proposed to interpret this kind of disordering. The simulated SAED patterns on the basis of the proposed atomic model agree with the experimental ones very well. This strong disorder may break both the coherence of the CDW along the chain direction and the phase order of the CDW in the transverse directions, and furthermore it may suppress the Peierls transition.

1. Introduction

The charge-density-wave (CDW) instabilities in low dimensional materials have ignited continued attention and interest for several decades (for example, refer to [1–34] and references therein). Recent developments ensure that the materials have potential applications [31–35]. The quasi-one-dimensional (1D) blue bronze $K_{0.3}MoO_3$ is one of the most studied CDW conductors [5–32].

[1] Author to whom any correspondence should be addressed.

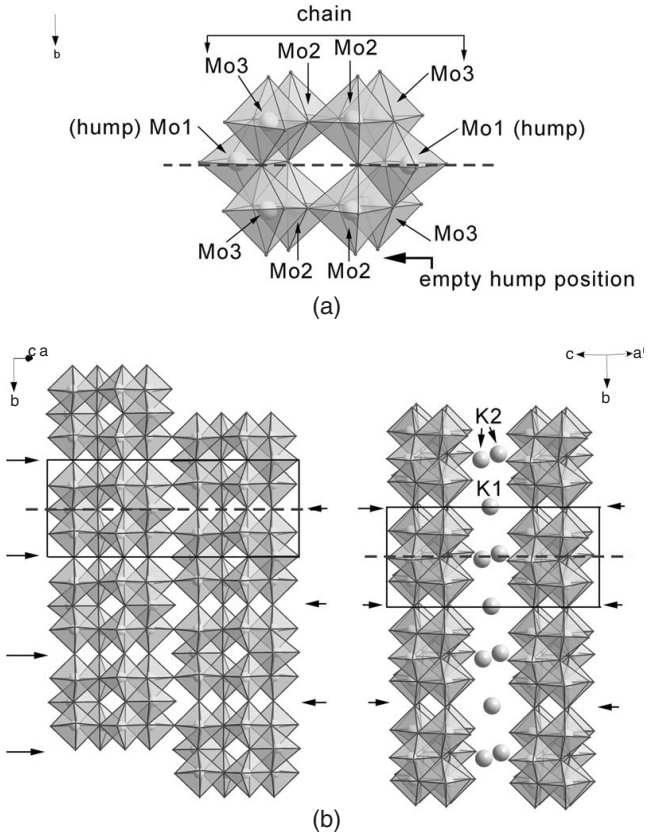

Figure 1. Schematic diagrams for the ordered structure of $K_{0.3}MoO_3$ by referring to [20–22]. (a) The $Mo_{10}O_{30}$ cluster. (b) The sheets of octahedral chains in the $(\bar{2}01)$ plane (left) and perspective view nearly along the [101] direction (right). (c) View along $[0\bar{1}0]$, showing two unit cells with double c. (d) Three-dimensional view of the chain of oxygen polyhedra around the K cations. In all the figures, characters attached to the atoms denote the types of the atoms according to [20], which is also listed in table 1 for comparison between the ordered and disordered atomic models. The arrows without characters indicate the empty positions which can be occupied by Mo1 octahedra randomly in the disordered state.

Before the CDW phenomenon was found in the $K_{0.3}MoO_3$ crystal [6], its crystal structure had been determined by Graham and Wadsley [20] and has been confirmed by several groups [21–23]. To clarify structural disordering studied in the present work, we draw some schematic diagrams for the structure of the blue bronze $K_{0.3}MoO_3$ in figure 1, based on the structural data provided mainly by Graham and Wadsley [20] and also by references [21, 22]. The differences of the structural data in references [20–22] do not matter to our result and clarification. The $K_{0.3}MoO_3$ crystal is monoclinic, space group $C2/m$ (no 12), with 20 formula units in a unit cell. The lattice parameters are $a = 18.249$ Å, $b = 7.560$ Å, $c = 9.855$ Å and $\beta = 117.32°$. Ten distorted MoO_6 octahedra, namely, four Mo2 and four Mo3 'chain' octahedra and two Mo1 'hump' octahedra as shown in figure 1(a), form a rigid unit (cluster), by sharing their edges or corners. These clusters are linked together to form chains by sharing corners O4 of the Mo2 and O7 of the Mo3 octahedra along the [010] direction. Hence Mo2 and Mo3 are called 'chain' octahedra; see the left- or right-hand side chain in the left part of figure 1(b). These chains are then linked together to form slabs (or sheets) by sharing corners

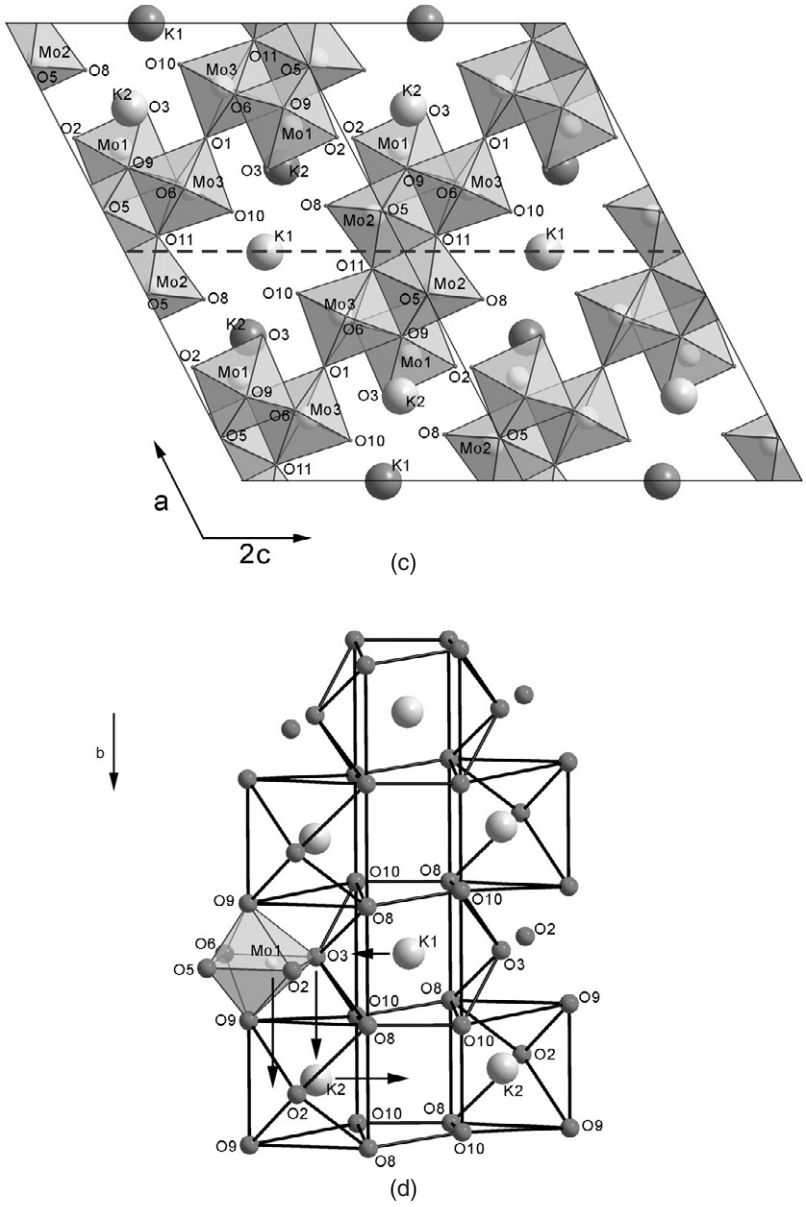

Figure 1. (Continued.)

O1 of the Mo3 octahedra along the [102] direction. Notice that there are two corners O1, belonging to two Mo3 octahedra with a separation of **b**/2, to be shared with the neighbour chain. According to the structural data provided by Graham and Wadsley [20], there should be a shift of **b**/2, namely, the upper O1 of the right-hand side chain is connected with the lower O1 of the left-hand side chain, as shown in figures 1(b) and (c). The Mo1 octahedra sharing two edges with the outer part of the chains are called 'hump' octahedra, which are indexed in figure 1(a). The empty 'hump' position means the position unoccupied by the Mo1 octahedron, which is designated by the arrow and characters in figure 1(a) and indicated by the arrows in

figure 1(b). These sheets formed by the chains are held together by the K^+ ions, situated at the centre of the O^{2-} polyhedra. The polyhedron for the K1 ion consists of a quadratic prism and two O3, and the polyhedron for the K2 ion consists of a trigonal prism and two O2. These K^+–O^{2-} polyhedra form the isolated one-dimensional chains of cages along the **b** direction without bridging laterally to adjacent chains; see figures 1(c) and (d).

The conductivity along the **b**-chain axis, along [102] and perpendicular to the octahedral slabs (i.e. $(\bar{2}01)$ plane) is different by several orders of magnitude [8], so that $K_{0.3}MoO_3$ is regarded as a 1D conductor along the **b** direction. Furthermore, it shows a metal–semiconductor transition, i.e. Peierls transition, at about 183 K [5–8, 10, 12]. At this temperature, the charge along **b** forms density wave simultaneously with lattice distortion, of which the modulation wavevector is $(1, 1 \pm q, -0.5)$ with q close to 0.25. Mo2 and Mo3 chain octahedra play an important direct role in the transition, while others have an indirect influence.

X-ray diffraction (XRD), x-ray diffuse scattering, neutron diffraction and scattering play very important roles in determining the microstructure of $K_{0.3}MoO_3$ at room temperature (RT) and the CDW at low temperature (LT) [7, 8, 12–15, 20–22, 24, 33]. Disorder and defects induced by doping and electron irradiation etc will suppress the Peierls transition and pin the CDW movement [7–9, 12–19]. Both localized disorder and the CDW state may be examined and imaged by scanning tunnelling microscopy (STM) [25–28] and transmission electron microscopy (TEM). In order to observe the CDW and image the microstructure, such as domain, inhomogeneity, local disorder etc, TEM is also used in this field [23, 29, 31, 37]. However, besides providing useful information, the electron beam used in a transmission electron microscope (also abbreviated as TEM) can cause temporary or permanent change in the structure of the specimen, especially alkali compounds and transition-metal oxides [36]. The CDW super-lattice spots in the selected area electron diffraction (SAED) patterns disappear in several seconds due to the higher sensitivity of the $K_{0.3}MoO_3$ to electron irradiation. No change of the underlying spots was observed [29]. A similar circumstance was also found in purple bronze $K_{0.9}Mo_6O_{17}$ [37]. According to the Schlenker group [7–9], the Peierls transition temperature of $K_{0.3}MoO_3$ lowers after electron irradiation. The greater the irradiation dose, the lower is the transition temperature. After annealing at 260 K, the transition temperature increases a little. The disorder induced by the irradiation may smear out the Peierls gap and suppress the Peierls transition.

In this paper, we report the structural disordering of the underlying lattice induced by electron irradiation in $K_{0.3}MoO_3$. This disordering is demonstrated clearly by the disappearance of the Bragg spots corresponding to the C-centre symmetry in the *in situ* recorded SAED patterns. The hypothetical simple atomic model for the disordered structure is proposed to interpret the experimental results.

2. Experimental details

The single crystals used in our experiments are prepared by the standard electrolytic reduction method from the molten salts of K_2CO_3–MoO_3 with an appropriate mole ratio [30]. The as-grown crystal is checked with the XRD and the perfect $K_{0.3}MoO_3$ crystallinity is confirmed, which is not presented here. The specimens used for transmission electron microscopy (TEM) study are mechanically thinned, dimpled and then ion-milled with a Gatan precision ion polishing system (PIPS). The film of the TEM specimen is parallel to the $(\bar{2}01)$ plane.

Before the *in situ* TEM experiment, the perfect C-centre ordered lattice of the specimen is confirmed by the high resolution transmission electron microscopy (HRTEM) technique in a JEOL JEM-2010FEF (UHR) TEM with the first 'F' denoting a Schottky type field emission gun (brightness $\sim 5 \times 10^8$ A cm^{-2} sr^{-1}), 'EF' the in-column Ω-type energy filter system and

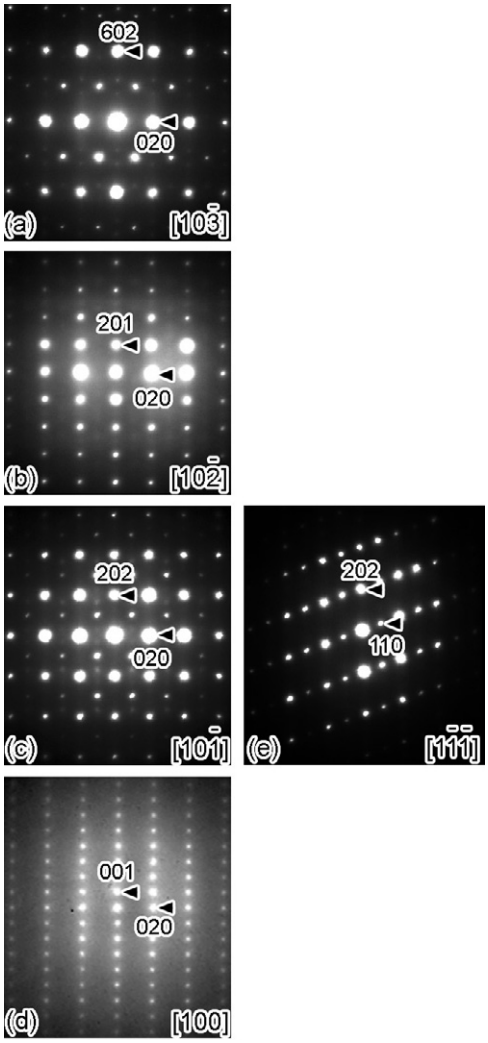

Figure 2. The SAED patterns recorded under RT before strong electron irradiation.

'UHR' the ultra-high resolution pole pieces. The HRTEM images are recorded on a model 794 multi-scan CCD camera with 1024 pixels × 1024 pixels.

Then, the *in situ* SAED observation is carried out in the JEOL JEM-2010 (HT) TEM with a thermionic LaB_6 electron gun (brightness $\sim 5 \times 10^6$ A cm^{-2} sr^{-1}) and high tilt (HT) pole pieces. The TEM acts as both the electron irradiation facility and the structural analysis and recording instrument. The SAED patterns are recorded on a model 780 dual-view CCD camera with 1300 pixels × 1030 pixels. A double tilt liquid nitrogen cooling sample holder (Gatan 636) is used and the temperature of the sample is decreased from room temperature (RT) to 230, 200, 170, 150, 120 K and finally 100 K step by step. It takes about 10 min to reach the next prefixed temperature. One temperature is maintained for about 20 min to observe and record the SAED patterns. With the time elapsing, the irradiation dose accumulates.

After the *in situ* SAED observation, the temperature of the sample is increased to RT and the sample is taken out for HRTEM examination of the disorder structure in the JEM-2010FEF TEM.

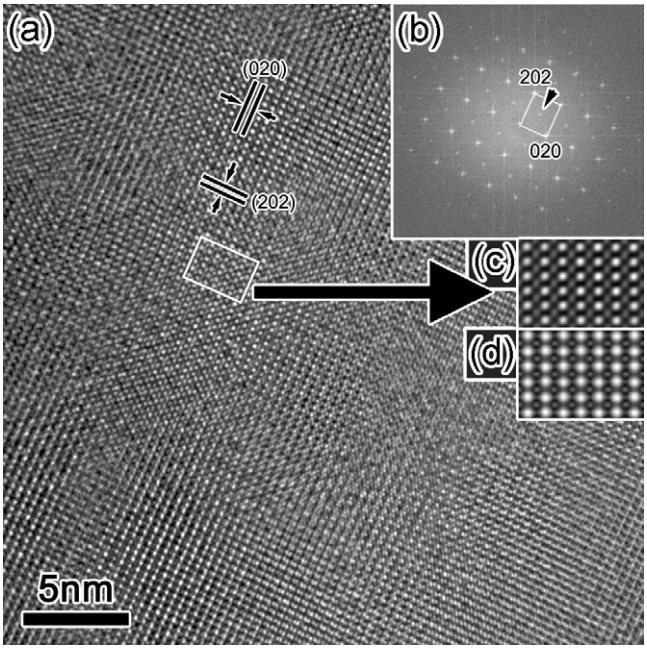

Figure 3. (a) The energy-filtered HRTEM image recorded along [10$\bar{1}$] under RT before strong electron irradiation. (b) FFT pattern of (a). (c) Zoomed HRTEM image taken from the framed region in (a), after Fourier filtering. (d) Simulated HRTEM image.

In all the TEM experiments, the acceleration voltage is 200 kV and the images are recorded with the aid of the Gatan DigitalMicrograph image acquisition and analysis software, which is also used to carry out the fast Fourier transformation (FFT) analysis for the HRTEM images. The simulation of SAED patterns and HRTEM images is carried out with JEOL MssC32 software.

3. Results

3.1. RT HRTEM and SAED observation

Under RT the SAED patterns are recorded, of which those along the [10$\bar{1}$], [10$\bar{2}$], [10$\bar{3}$], [100], and [1$\bar{1}\bar{1}$] zone axes are shown in figure 2. The SAED patterns are indexed on the basis of the $K_{0.3}MoO_3$ crystal structure proposed by Graham and Wadsley [20]. The patterns show that the $K_{0.3}MoO_3$ crystal possesses perfect C-centre symmetry before strong electron irradiation damage. The reflections (111) in the [10$\bar{1}$] SAED pattern shown in figure 2(c) and (311) in the [10$\bar{3}$] pattern shown in figure 2(a) denote the C-centre symmetry.

Figure 3(a) is one zero-loss energy filtered HRTEM image along the [10$\bar{1}$] axis under RT, the FFT pattern of which is shown in the inset figure 3(b). Normally, the FFT pattern of the HRTEM image along one zone axis has the same characteristics and meaning as the SAED pattern recorded along the same axis. So, the FFT image in figure 3(b) resembles the [10$\bar{1}$] SAED shown in figure 2(c) completely. The spot indicated by the arrowhead in the centre of the rectangle in the FFT pattern of figure 3(b), namely, the (111) reflection denoting the C-centre symmetry, can also be clearly seen. The zoomed HRTEM image shown as the inset in figure 3(c) taken from the framed region in figure 3(a), after Fourier filtering, agrees very

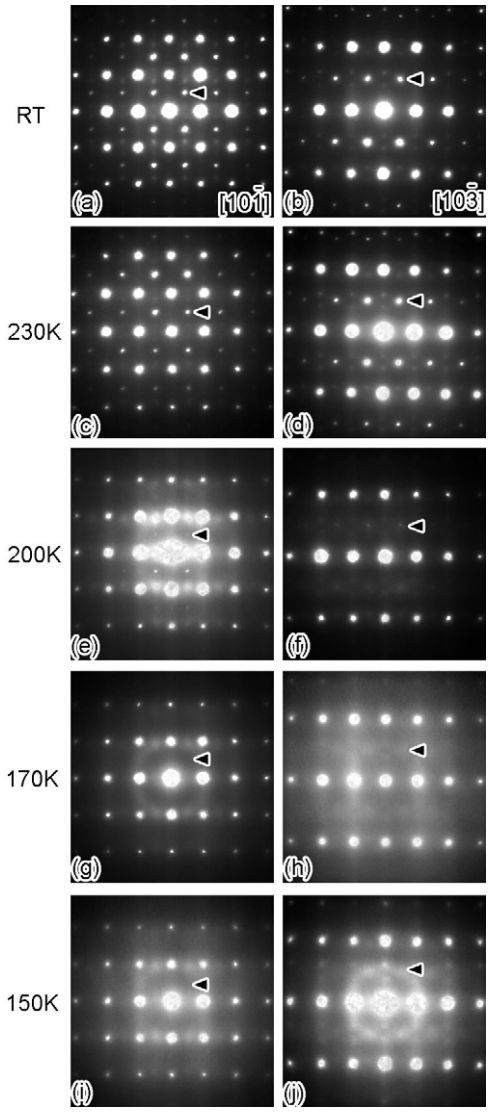

Figure 4. A series of *in situ* recorded SAED patterns, when temperature is lowered, along [10$\bar{1}$] (a), (c), (e), (g), (i) and [10$\bar{3}$] directions (b), (d), (f), (h), (j) respectively.

well with the simulated HRTEM image shown as the inset in figure 3(d), based on the C-centre $K_{0.3}MoO_3$ crystal structure data given by Graham and Wadsley [20]. These results confirm the C-centre order of the $K_{0.3}MoO_3$ crystal in direct space again, in addition to the verification in the reciprocal space as shown in figures 2(a) and (c). Furthermore, figure 3(a) shows the perfect ordered structure nearly everywhere in the sample before strong irradiation damage.

3.2. In situ SAED observation and structural disordering

We present a series of the *in situ* recorded SAED patterns along [10$\bar{1}$] (figures 4(a), (c), (e), (g), (i)) and [10$\bar{3}$] (figures 4(b), (d), (f), (h), (j)) zone axes from the same region of the sample under RT, 230, 200, 170, and 150 K in figure 4. From these SAED patterns, we can see clearly that both the (111) reflection in the [10$\bar{1}$] pattern and (311) in the [10$\bar{3}$] pattern (indicated by arrow heads) significantly change from acute and bright spots to blurred ones, and finally

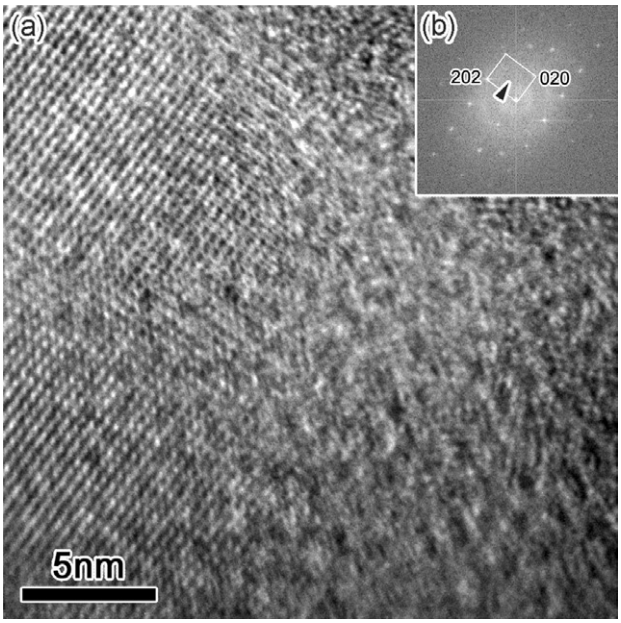

Figure 5. (a) The energy-filtered HRTEM image recorded along [10$\bar{1}$] under RT after strong electron irradiation at LT. (b) FFT pattern of (a).

disappear completely, with temperature decreasing and electron irradiation dose accumulating. In contrast to these, the other spots remain nearly unchanged. These important results indicate that the underlying lattice of $K_{0.3}MoO_3$ undergoes a structural disordering during the strong electron irradiation. The C-centre long range order is destroyed and the underlying structure becomes a disordered one without C-centre symmetry. From figure 4, we can see that the blurred diffraction ring from amorphous structure gradually appear as well after long time irradiation dose accumulation. We also find that the damaged structure cannot be recovered by atomic thermal vibration under LT, that is to say, electron irradiation can damage the lattice much more easily under LT than RT.

To obtain a more direct impression of the damaged lattice structure, we increased the temperature to RT gradually and used a JEM-2010FEF TEM to observe the HRTEM images for the damaged region of the sample along the [10$\bar{1}$] zone axis. The result is shown as figure 5(a), from which we can see that the lattice is not as perfect as that before strong irradiation shown in figure 3(a) and some areas have become completely amorphous. The FFT pattern from figure 5(a), shown as the inset in figure 5(b), reveals that the (111) spot disappears with others remaining, similar to the results from SAED observation. This also confirms that the post-irradiation lattice loses the C-centre order and the damage of the structure cannot be recovered by increasing the temperature to RT. The *in situ* heating TEM experiment is to be carried out.

4. Discussion

4.1. Schematic demonstration of structural disordering

To illustrate the structural disordering observed in the experiment, we draw the schematic two-dimensional pictures in both the direct space and reciprocal space showing the ordered and disordered structures as figure 6. Figure 6(a) shows the ordered structure, in which there are

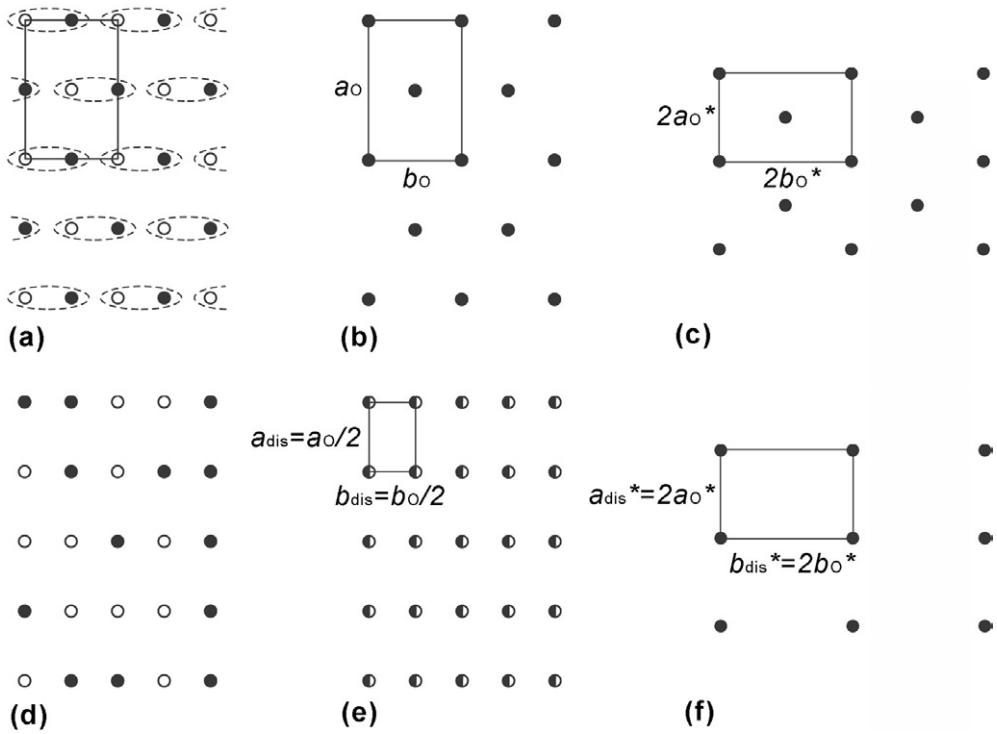

Figure 6. Schematic diagram illustrating the structural disordering. (a) Atomic model consisting of two ordered blocks (solid and open circles), where the unit cell is the ellipse including two ordered blocks. (b) The lattice in direct space for ordered structure, where $\mathbf{a}_o$ and $\mathbf{b}_o$ denote the basis vectors of the unit cell. (c) The reciprocal lattice for ordered structure, where $\mathbf{a}_o^*$ and $\mathbf{b}_o^*$ denote reciprocal basis vectors for ordered structure. (d) Atomic model consisting of two randomly distributed blocks (solid and open circles). (e) The statistical model for the disordered structure in (d). Here the unit cell is one unit by mixing the two blocks (50% solid and 50% open circles), of which the basis vectors are $\mathbf{a}_{dis} = \mathbf{a}_o/2$ and $\mathbf{b}_{dis} = \mathbf{b}_o/2$. (f) The corresponding reciprocal lattice for the disordered structure, where $\mathbf{a}_{dis}^* = 2\mathbf{a}_o^*$ and $\mathbf{b}_{dis}^* = 2\mathbf{b}_o^*$ are the basis vectors.

two basic units (solid circle and open circle) arranged in ordered sequence. The open ellipse, with the two ordered units inside, can be chosen as a unit cell to form the centred lattice in direct space, shown as figure 6(b). The basis vectors are a_o and b_o. Correspondingly, in figure 6(c), the reciprocal space of the ordered lattice also shows the centre symmetry with the two reciprocal basis vectors a_o^* and b_o^*. After strong electron irradiation, the ordered structure is destroyed and the two basic units (solid circle and open circle) become randomly distributed, forming a disordered lattice (figure 6(d)). We draw a statistically disordered model lattice as figure 6(e) to represent this random disorder. The basis vectors are $a_{dis} = a_o/2$ and $b_{dis} = b_o/2$. Figure 6(f) shows the corresponding reciprocal space for the disordered structure, with the reciprocal $a_{dis}^* = 2a_o^*$ and $b_{dis}^* = 2b_o^*$, which show no centre symmetry. This can interpret the observation of the structural disordering.

4.2. Hypothetical atomic model for disordered structure

Based on the above explanation and the crystal structure of $K_{0.3}MoO_3$ provided by Graham and Wadsley [20], we propose an atomic model to statistically depict the disordered structure,

Table 1. Crystal data and fractional atomic coordinates of the hypothetical disordered model.

Crystallographic data						
Crystal system	Monoclinic					
Space group	$P12/m1$ (no 10)					
Unit cell dimensions	$a = 9.1245$ Å					
	$b = 3.7800$ Å					
	$c = 9.8550$ Å					
	$\beta = 117.32°$					
Fractional atomic coordinates						
			Coordinates			
Atom	Multiplicity and Wyckoff letter	Occupancy	x	y	z	Ordered atom[a]
K1	1*c*	0.5	0	0	1/2	K1
K2	2*m*	0.5	0.6347	0	0.3105	K2
Mo1	2*m*	0.5	0.4514	0	0.1732	Mo1
Mo2	2*n*	1	0.8416	1/2	0.0430	Mo2
Mo3	2*n*	1	0.2762	1/2	0.3464	Mo3
O1	1*h*	1	1/2	1/2	1/2	O1
O2	2*m*	0.5	0.4982	0	0.0284	O2
O3	2*m*	0.5	0.6347	0	0.3105	O3
O4	2*m*	1	0.8155	0	0.0052	O4, O5
O5	2*m*	1	0.2955	0	0.3217	O6, O7
O6	2*n*	1	0.7958	1/2	0.1939	O8
O7	2*n*	1	0.3682	1/2	0.1650	O9
O8	2*n*	1	0.1786	1/2	0.4573	O10
O9	2*n*	1	0.0722	1/2	0.1455	O11

[a] The corresponding atom symbols in the ordered crystal structure given by Graham and Wadsley [20].

which is shown in table 1. The relationship between the basis vectors for the new disordered unit cell and those for the ordered one is the following: $a_{dis} = a_o/2$, $b_{dis} = b_o/2$ and $c_{dis} = c_o$. That is to say, the unit cell of the ordered $K_{0.3}MoO_3$ is divided into four parts, each of which denotes a disordered unit cell without C-centre symmetry (figure 1).

In detail, we can divide the unit consisting of ten octahedra into two along the *b* axis. A dashed line is drawn to show the division in figures 1(a) and (b). As shown in figure 1(c), the unit cell can be divided into two along the *a* axis accordingly, so a dashed line denoting the division is also drawn. The unit cell along the *c* axis remains unchanged. This adjustment of atoms accords with the schematic illustration (figure 6) very well.

By mainly referring to [20–22, 38], the adjustment of the atoms is possible in the following way (see figure 1). Under electron irradiation, the K2 can occupy the big empty adjacent polyhedron cage first (indicated by the arrow in figure 1(d)). Simultaneously, Mo1 and O3 jump down to form a new octahedron in the empty 'hump' position. The K1 move to the vacant O3 position to maintain the local electrostatic balance.

Therefore, the atomic sites in the new unit cell for the disordered structure shown in table 1 could be obtained by the above division of the old ordered unit cell and slight adjustment of the K1, K2, Mo1, and O3 atoms.

Based on our new disordered atomic model, we calculate the SAED patterns along $[10\bar{1}]_o$ (i.e., $[20\bar{1}]_{dis}$) and $[10\bar{3}]_o$ (i.e., $[20\bar{3}]_{dis}$) zone axes shown respectively as figures 7(c) and (d), which possess no C-centre order and agree with the experimental results (figures 4(g), (i)

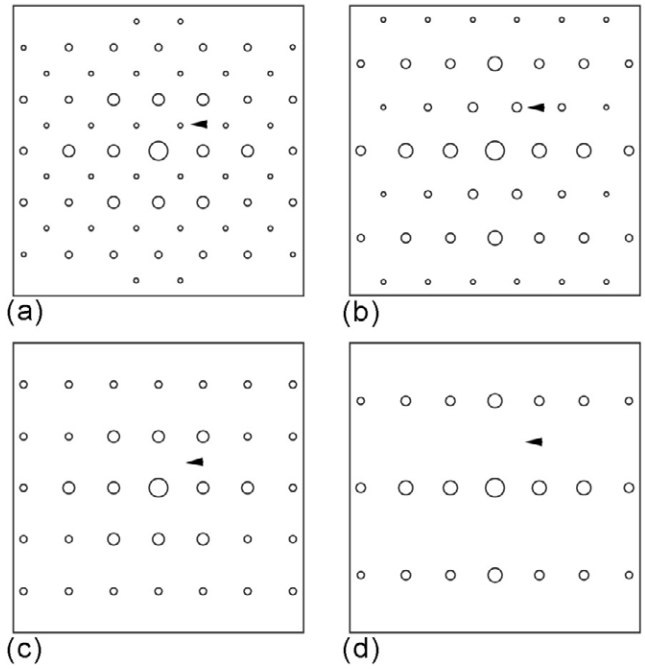

Figure 7. The calculated SAED patterns along (a) $[10\bar{1}]_o$ and (b) $[10\bar{3}]_o$ for the ordered structure based on the crystal data provided by Graham and Wadsley [20]. The calculated SAED patterns along (c) $[10\bar{1}]_o$ (i.e., $[20\bar{1}]_{dis}$) and (d) $[10\bar{3}]_o$ (i.e., $[20\bar{3}]_{dis}$) for the disordered structure based on our atomic model shown in table 1. The arrowheads indicate the positions of the reflections representing the C-centre symmetry.

and 4(h), (j)). In order to compare conveniently, we still use the reciprocal index system of the ordered structure. To compare, we also calculate the SAED patterns of the ordered structure along the $[10\bar{1}]$ and $[10\bar{3}]$ zone axes shown respectively as figures 7(a) and (b) based on the crystal structure provided by Graham and Wadsley [20]. The patterns in figures 7(a) and (b) show the C-centre symmetry ((111) and (311) spots respectively) clearly; these resemble the experimental ones (figures 4(a), (c) and 4(b), (d)) completely. Our disordered atomic model is verified by the above comparison between the simulation and the experiment.

Chen *et al* [29] have not observed the change of the diffraction spots corresponding to the underlying lattice, which may be due to not too strong irradiation as well. In the strong irradiation case as stated in this paper, we observed the structural transition of the underlying lattice clearly.

5. Conclusion

In summary, we report that the structural disordering corresponding to the disappearance of C-centre symmetry of underlying lattice induced by electron irradiation in $K_{0.3}MoO_3$ blue bronze. This disordering is demonstrated clearly from the *in situ* recorded SAED patterns in the TEM. The hypothetical atomic model for the disordered structure is proposed and used to simulate the SAED patterns, which agree with the experimental ones very well. This disordering may suppress the Peierls transition.

Acknowledgments

This work was supported by the National Natural Science Foundation of China (grant Nos 10404020, 10474074 and 10174056) and Wuhan University Innovation Fund for Natural Science.

References

[1] Salvo F J D Jr and Rice T M 1979 *Phys. Today* **32** 32
[2] Thorne R E 1996 *Phys. Today* **49** 42
[3] Brown S and Grüner G 1994 *Sci. Am.* **270** 28
[4] Grüner G 1988 *Rev. Mod. Phys.* **60** 1129
[5] Schlenker C, Dumas J, Greenblatt M and van Smaalen S (ed) 1996 *Physics and Chemistry of Low-Dimensional Inorganic Conductors* (New York: Plenum)
[6] Pouget J P, Kagoshima S, Schlenker C and Marcus J 1983 *J. Phys. Lett.* **44** L113
[7] Schlenker C and Dumas J 1986 *Crystal Chemistry and Physical Properties of Quasi 1D Structures* ed J Rouxel (Dordrecht: Reidel) p 135
[8] Rouxel J and Schlenker C 1989 *Charge Density Waves in Solids—Modern Problems in Condensed Matter Sciences* vol 25, ed L P Gor'kov and G Grüner (Amsterdam: North-Holland) p 15
[9] Mutka H, Bouffard S, Dumas J and Schlenker C 1984 *J. Phys. Lett.* **45** L729
[10] Dumas J, Schlenker C, Marcus J and Buder R 1983 *Phys. Rev. Lett.* **50** 757
[11] Sato M, Fujishita H and Hosnino S 1983 *J. Phys. C: Solid State Phys.* **16** L877
[12] Pouget J P and Comes R 1989 *Charge Density Waves in Solids—Modern Problems in Condensed Matter Sciences* vol 25, ed L P Gor'kov and G Grüner (Amsterdam: North-Holland) p 85
[13] Rouzière S, Ravy S and Pouget J P 1995 *Synth. Met.* **70** 1259
[14] Rouzière S, Ravy S, Pouget J P and Brazovskii S 2000 *Phys. Rev.* B **62** R16231
[15] Rouzière S, Ravy S and Pouget J P 1997 *Synth. Met.* **86** 2131
[16] Shi J, Tian M L, Xia H B, Zhu J S, Wu J X, Tian D C and Zhang Y H 1995 *Solid State Commun.* **95** 625
[17] Tian M L, Mao Z Q, Zhang Y H, Shi J and Tian D C 1994 *Phys. Rev.* B **49** 2306
[18] Wang D L, Xiao Q M, Tang W F, Zhao T Y, Shi J, Tian D C and Tian M L 1999 *Mod. Phys. Lett.* B **13** 109
[19] Zhuang Z Z, Wang K Q, Chen Z J, Cao L Z, Tian M L, Zhang Y H and Junod A 1996 *Solid State Commun.* **99** 265
[20] Graham J and Wadsley A D 1966 *Acta Crystallogr.* **20** 93
[21] Ghedira M, Chenavas J, Marezio M and Marcus J 1985 *J. Solid State Chem.* **57** 300
[22] Schutte W J and de Boer J L 1993 *Acta Crystallogr.* B **49** 579
[23] Li H L, Zou H M, Wen J G and Tian M L 1993 unpublished
[24] Tian M L, Chen L and Zhang Y H 2000 *Phys. Rev.* B **62** 1504
[25] Anselmetti D, Wiesendanger R, Güntherodt H-J and Grüner G 1990 *Europhys. Lett.* **12** 241
[26] Heil J, Wesner J, Lommel B, Assmus W and Grill W 1989 *J. Appl. Phys.* **65** 5220
[27] Rudd G, Novak D, Saulys D, Bartynski R A, Garofalini S, Ramanujachary K V, Greenblatt M and Garfunker E 1991 *J. Vac. Sci. Technol.* B **9** 909
[28] Walter U, Thomson R E, Burk B, Crommie M F, Zettl A and Clarke J 1992 *Phys. Rev.* B **45** 11474
[29] Chen C H, Schneemeyer L F and Fleming R M 1984 *Phys. Rev.* B **29** 3765
[30] Huang Z, Tian M L and Tian D C 1990 *Chin. J. Low Temp. Phys.* **12** 78
[31] Ogawa N, Murakami Y and Miyano K 2002 *Phys. Rev.* B **65** 155107
[32] Ogawa N, Shiraga A, Konda R, Kagoshima S and Miyano K 2001 *Phys. Rev. Lett.* **87** 256401
[33] Mantel O C, van der Zant H S J, Steinfort A J, Træholt C and Dekker C 1997 *Synth. Met.* **86** 2193
[34] van der Zant H S J, Mantel O C, Dekker C, Mooij J E and Træholt C 1996 *Appl. Phys. Lett.* **68** 3823
[35] Steinfort A J, van der Zant H S J, Smits A B, Mantel O C, Scholte P M L O and Dekker C 1998 *Phys. Rev.* B **57** 12530
[36] Egerton R F, Li P and Malac M 2004 *Micron* **35** 399
[37] Escribe-Fillippinin C, Konaté K, Marcus J, Schlenker C, Almairac R, Ayroles R and Roucau C 1984 *Phil. Mag.* B **50** 321
[38] Shannon R D 1976 *Acta Crystallogr.* A **32** 751